

Fermi National Accelerator Laboratory

FERMILAB-Conf-96/192-E

D0

Top Production at D0

Meenakshi Narain

For the D0 Collaboration

*Fermi National Accelerator Laboratory
P.O. Box 500, Batavia, Illinois 60510*

August 1996

Presented at the 1996 Rencontre de Physique de la Vallee d'Aoste on Results and Perspectives in Particle Physics, La Thuile, Italy, March 4-9, 1996

Disclaimer

This report was prepared as an account of work sponsored by an agency of the United States Government. Neither the United States Government nor any agency thereof, nor any of their employees, makes any warranty, expressed or implied, or assumes any legal liability or responsibility for the accuracy, completeness, or usefulness of any information, apparatus, product, or process disclosed, or represents that its use would not infringe privately owned rights. Reference herein to any specific commercial product, process, or service by trade name, trademark, manufacturer, or otherwise, does not necessarily constitute or imply its endorsement, recommendation, or favoring by the United States Government or any agency thereof. The views and opinions of authors expressed herein do not necessarily state or reflect those of the United States Government or any agency thereof.

FERMILAB CONF-96/192-E

TOP PRODUCTION at DØ¹

Meenakshi Narain

*Fermi National Accelerator Laboratory
P. O. Box 500
Batavia, IL 60510*

For the DØ Collaboration

Abstract

We report an updated measurement of the top quark production cross section in $p\bar{p}$ collisions at $\sqrt{s} = 1.8$ TeV by the DØ experiment at the Fermilab Tevatron. We also present a measurement of the top quark mass. The data set used for these measurements corresponds to approximately 100 pb^{-1} , almost the entire data sample collected by the DØ experiment during the Run I of the Fermilab Tevatron. We observe 37 events with an expected background of 13.4 ± 3.0 events. We measure the mass of the top quark to be $170 \pm 15(\text{stat.}) \pm 10(\text{syst.}) \text{ GeV}/c^2$. At this mass we find the top production cross section to be $5.2 \pm 1.8 \text{ pb}$.

¹presented at the 1996 Rencontre de Physique de la Vallée d'Aoste on Results and Perspectives in Particle Physics, La Thuile, Italy, March 4–9, 1996.

1 Introduction

The discovery of the top quark in 1995 by the DØ[1] and CDF[2] collaborations at the Fermilab Tevatron collider ended a two decade long search which began soon after the discovery of the b quark. The top quark completes the three quark families and its discovery represents another triumph of the Standard Model. Its large mass at the same time draws attention to the area of the Standard Model that is least understood, the mechanism of electroweak symmetry breaking and the fermion masses.

Presently, only the Fermilab Tevatron, which collides protons and antiprotons at a center of mass energy of $\sqrt{s} = 1.8$ TeV, has sufficient energy to produce top quarks. Since the observation of the top quark was reported last year, the DØ experiment has doubled its data sample. The goal is now to measure the $t\bar{t}$ production cross section and the properties of the top quark as well as possible. In this report we present our updated measurement of the production cross section and the mass of the top quark from ≈ 100 pb $^{-1}$ of data collected during two collider running periods, Run 1a (1992–93) and Run 1b (1994–1995).

At the Fermilab Tevatron top quarks are predominantly pair produced through $q\bar{q}$ annihilation or gluon fusion. Due to its large mass the top quark decays before it hadronizes. It is expected to decay almost all the time to a W boson and a b quark ($\sim 99.8\%$), allowing for an extremely small contribution for the CKM suppressed decay modes $t \rightarrow W + s$ and $t \rightarrow W + d$. Depending on the subsequent decay mode of the W ($W \rightarrow \ell\nu$ or $W \rightarrow q\bar{q}$), we distinguish three major signatures of $t\bar{t}$ decays:

- A. *Dilepton channel*: both W s decay leptonically to $e\nu$ or $\mu\nu$. The branching fraction for this mode is rather small (4/81), but it has the advantage of extremely small backgrounds.
- B. *Lepton+jets channel*: one W decays leptonically to $e\nu$ or $\mu\nu$ and the other hadronically. The branching fraction is 24/81. The dominant source of background for this mode is W +jets production. We further distinguish the b tagged lepton+jets channel, in which a muon from the semileptonic decay of a b quark was detected (ℓ +jets/ μ), and the topological lepton+jets channel, in which the topology of the event is top-like and no b was tagged (ℓ +jets.).
- C. *All jets channel*: both W s decay hadronically. This channel has the highest branching fraction (36/81), but is swamped by background from multijet production.

At the moment, we ignore decays with τ leptons in the final state. Work on these channels is in progress.

A detailed description of the DØ detector can be found elsewhere [3]. Trigger and reconstruction algorithms for jets and missing transverse energy have been described in previous publications [4]. The electron and muon identification algorithms have been improved. Electrons are clusters of electromagnetic energy, characterized by a number of variables that describe the shower shape and the associated charged track. We select clusters based on the ratio of the joint likelihood of these variables for electrons and backgrounds. Using the joint likelihood rather than cutting on individual variables reduced the multi-jet background by a factor of 2. The electron finding efficiency was measured using $Z \rightarrow ee$ data. The muon identification has been refined by the use of the finely segmented calorimeter to discriminate between prompt muons from the $p\bar{p}$ interaction, cosmic rays and combinatoric backgrounds, resulting in a factor 2 reduction in background and a 20% improvement in efficiency.

2 Dilepton Mode

The signature for dilepton decays is two isolated high- p_T leptons, two or more jets and large \cancel{p}_T . The basic selection criteria are summarized in Table 1. Some cuts to remove specific backgrounds are omitted from the table for simplicity. H_T is the sum of all jet p_{Ts} and the p_T of the leading electron. In the case of the $\mu\mu$ channel it is only the sum of the jet p_{Ts} . Figure 1 shows the expected and observed H_T spectra. The table also lists the number of events observed and the expected number of background and signal[5] events.

For the dilepton channels as well as all of the other analyses reported in this paper the percentage of $t\bar{t}$ events expected to pass the selection criteria was calculated for various top quark masses between 120 and 200 GeV/ c^2 using samples of $t\bar{t}$ decays to all allowed final states, produced with the ISAJET event generator[7] and a GEANT[8] model of the DØ detector. The Monte Carlo events were selected according to the same criteria as the data. The errors quoted on the expected number of signal events include the effects of varying the jet energy scale by one standard deviation, differences between HERWIG[9] and ISAJET event generators, uncertainties in the muon momentum resolution, trigger and lepton identification efficiencies.

We distinguish between physics backgrounds because they have the same final state as the signal process, and instrumental backgrounds in which the final state was misidentified.

The main physics backgrounds are Z and continuum Drell-Yan production ($Z, \gamma^* \rightarrow ee, \mu\mu$, and $\tau\tau$), vector boson pairs (WW, WZ), and heavy flavor ($b\bar{b}$ and $c\bar{c}$) production. The large $Z \rightarrow ee$ background in the ee channel is rejected by tightening the cut on \cancel{p}_T if the dielectron mass is close to the Z mass. In the $\mu\mu$ channel, Z decays are removed by a

Table 1: Summary of dilepton channel.

channel	$e\mu$	ee	$\mu\mu$
lepton p_T	> 15 GeV	> 20 GeV	> 15 GeV
electron $ \eta $	< 2.5	< 2.5	—
muon $ \eta $	< 1.7	—	< 1.0
\cancel{p}_T	> 20 GeV	> 25 GeV	—
jet p_T	> 20 GeV	> 20 GeV	> 20 GeV
jet $ \eta $	< 2.5	< 2.5	< 2.5
H_T	> 120 GeV	> 120 GeV	> 100 GeV
$\int \mathcal{L} dt$	91 pb ⁻¹	106 pb ⁻¹	87 pb ⁻¹
events observed	3	1	1
background	0.36 ± 0.09	0.66 ± 0.17	0.55 ± 0.28
signal ($m_t = 150$ GeV)	3.40 ± 0.55	1.99 ± 0.25	0.92 ± 0.19
($m_t = 180$ GeV)	1.69 ± 0.27	0.92 ± 0.11	0.53 ± 0.11
($m_t = 200$ GeV)	1.00 ± 0.16	0.59 ± 0.07	0.27 ± 0.06

kinematic fit to the $Z \rightarrow \mu\mu$ hypothesis. These backgrounds were estimated by a Monte Carlo simulation, augmented by efficiencies measured from the collider data.

Instrumental backgrounds in the $e\mu$ +jets and ee +jets channels due to jets misidentified as electrons were estimated entirely from data using control samples to measure the jet misidentification probability (typically 2×10^{-4}). For muons instrumental backgrounds (*e.g.* hadronic punchthrough and cosmic rays) were found to be negligible.

3 Lepton+jets mode

3.1 Event selection criteria

The signature of this mode consists of one isolated high p_T lepton, \cancel{p}_T due to the neutrino and a number of jets. In these decays jets are produced in the hadronization of the the two b quarks and the quarks from W decay. Due to gluon radiation and detector effects more or less than four jets may actually be detected. Therefore the number of jets required is analysis dependent.

Figure 2 shows the jet multiplicity spectrum in events selected with the requirement of one isolated high p_T lepton and \cancel{p}_T . We compare this to the jet multiplicity spectrum expected for a simulated sample of $t\bar{t}$ events with a mass of 180 GeV. The top sample is

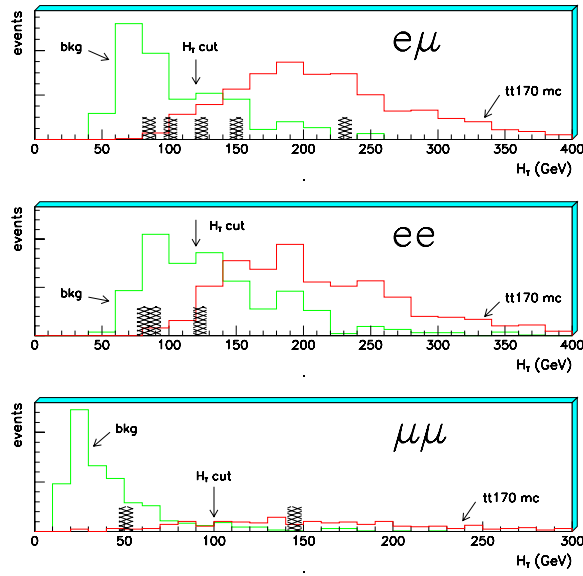


Figure 1: H_T distribution of Dilepton events. The open histograms show the expected distributions for $t\bar{t}$ events for $m_t = 170$ GeV (tt170 mc) and for background (bkg). The crosshatched histograms show the H_T values for the events in our data sample before the H_T cut..

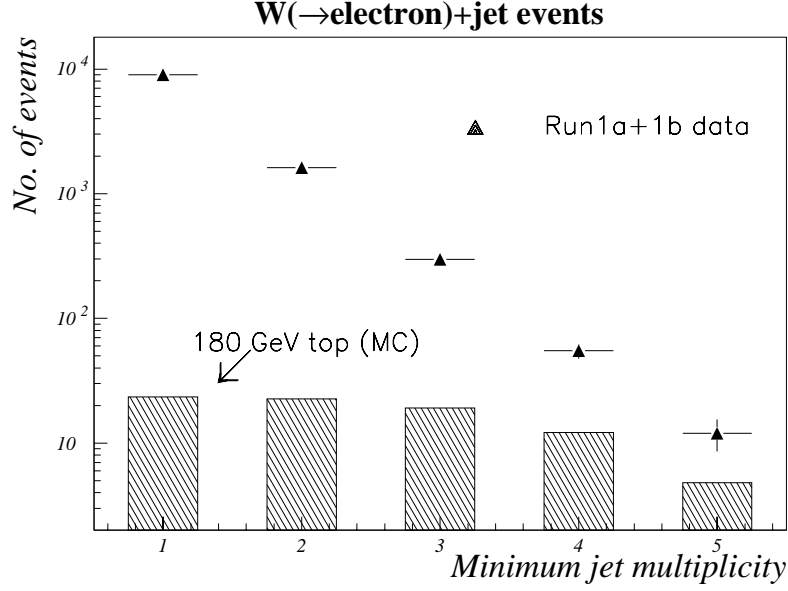


Figure 2: Jet Multiplicity distribution in e +jets events.

absolutely normalized assuming the calculated cross section [5]. Note that at this stage of the event selection the event sample is dominated by $W(\rightarrow \ell + \nu)$ +jets events, even at high jet multiplicities (≥ 3 or 4). In order to enhance the relative contribution of events from top quark decays additional rejection power against backgrounds is needed. We employ two techniques to achieve this. One method tags a b quark jet in the event by its semileptonic decay ($b \rightarrow \mu + X$). The other method exploits the difference in event shapes between $t\bar{t}$ and background events. We call this the topological analysis. All events that satisfy the b tag selection are excluded from the topological analysis, in order to keep the two event samples mutually exclusive.

Both methods rely on event shape variables to discriminate against backgrounds, but the requirements are looser in the case of the b tag analysis. In order to determine the event shape variables and cut values that give us the best precision on the measured cross section we performed an optimization, using the Random Grid Search technique[10]. In the optimization procedure we studied a number of different selection variables:

- $\mathcal{A}(W + \text{jets})$, the aplanarity computed using the W and jet momenta in the laboratory frame[11];
- $\mathcal{A}(\text{jets})$, the aplanarity computed using the jet momenta only;
- \cancel{p}_T ;

- $p_T(W)$, the transverse momentum of the W ;
- H_T , the scalar sum of the p_T of all jets;
- $H_T + p_T(W)$;
- $(p_T(\ell) + \cancel{p}_T)/(H_T + p_T(W))$;
- number of jets.
- etc.

We used a Monte Carlo $t\bar{t}$ sample generated with $m_t = 180$ GeV to compute the expected signal event yield. To simulate the background we used the appropriate combinations of W +jets and multijet background data. For the ℓ +jets analysis the W +jets background was generated with VECBOS, the multijet background was taken from a control data sample. For the ℓ +jets/ μ analysis all background samples were derived from data. An integrated luminosity of 77pb^{-1} was assumed.

We then determined the expected number of signal and background events for a wide range of cuts on the above variables. In figure 3 every point represents a particular set of cuts on H_T and $\mathcal{A}(W + \text{jets})$. A boundary on which that the expected signal is maximized for a given background level is visible. It defines a family of threshold values. The variables $\mathcal{A}(W + \text{jets})$ and H_T give the best signal to noise ratio for a given signal efficiency. We then choose the set of cuts for which we predict the smallest uncertainty in the cross section measurement. This is achieved by comparing the optimal boundary curve to a set of contours which give us constant error in the top production cross section, with the goal of minimizing the error on the cross section measurement as well as contours of constant expected statistical significance. The selection criteria are given in table 2.

3.2 Lepton+jets topological analysis

Table 2 lists the selection criteria for the e +jets and μ +jets channels. After all cuts we observe 10 e +jets and 11 μ +jets events. Plots of $\mathcal{A}(W + \text{jets})$ vs. H_T after all cuts except on the variables plotted, for our data sample, W +jets, top MC($m_t = 180$ GeV) and multijet QCD background are shown in figure 4.

There are two main sources of background to the $t\bar{t}$ signal, W +jets production and multijet events with fake leptons and mismeasured \cancel{p}_T . We estimate the multijet background from a control multijet data sample. A detailed description of this method can be found in reference [4].

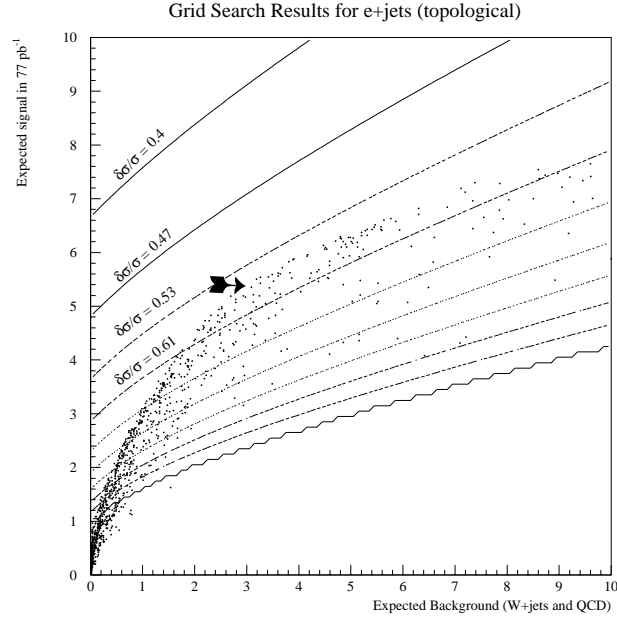


Figure 3: Grid Search results for $e + jets$ channel using variables H_T and $\mathcal{A}(W + jets)$. The set of curves overlaid represent contours of constant error in the top production cross section. The arrow points to the set of cuts used in the $e+jets$ analysis.

Table 2: Summary of Lepton+jets Channels.

channel	$e+\text{jets}$	$\mu+\text{jets}$	$e+\text{jets}/\mu$	$\mu+\text{jets}/\mu$
lepton p_T	$> 20 \text{ GeV}$	$> 20 \text{ GeV}$	$> 20 \text{ GeV}$	$> 20 \text{ GeV}$
lepton $ \eta $	< 2	< 1.7	< 2	< 1.7
\cancel{p}_T	$> 25 \text{ GeV}$	$> 20 \text{ GeV}$	$> 20 \text{ GeV}^\dagger$	$> 20 \text{ GeV}^\ddagger$
number of jets	≥ 4	≥ 4	≥ 3	≥ 3
jet p_T	$> 15 \text{ GeV}$	$> 15 \text{ GeV}$	$> 20 \text{ GeV}$	$> 20 \text{ GeV}$
jet $ \eta $	< 2	< 2	< 2	< 2
tagging μ^*	none	none	≥ 1	≥ 1
$p_T(\ell) + \cancel{p}_T$	$> 60 \text{ GeV}$	$> 60 \text{ GeV}$	—	—
$\mathcal{A}(W + \text{jets})$	> 0.065	> 0.065	> 0.04	> 0.04
H_T	$> 180 \text{ GeV}$	$> 180 \text{ GeV}$	$> 110 \text{ GeV}$	$> 110 \text{ GeV}$
$\int \mathcal{L} dt$	106 pb ⁻¹		96 pb ⁻¹	
events observed	21		11	
backgrounds ($W + \text{jets}$)	7.68 ± 2.77		1.84 ± 0.39	
(multijet)	1.55 ± 0.49		0.62 ± 0.20	
($Z \rightarrow \mu\mu$)	—		0.12 ± 0.06	
total	9.23 ± 2.83		2.58 ± 0.57	
signal ($m_t = 140 \text{ GeV}$)	31.90 ± 5.92		12.46 ± 2.67	
($m_t = 160 \text{ GeV}$)	18.84 ± 3.31		8.97 ± 2.21	
($m_t = 180 \text{ GeV}$)	12.87 ± 2.32		5.20 ± 1.28	
($m_t = 200 \text{ GeV}$)	7.72 ± 1.37		3.44 ± 0.88	

$^\dagger > 35 \text{ GeV}$ if $\Delta\phi(\cancel{p}_T, \mu) < 25^\circ$

$^\ddagger \Delta\phi(\cancel{p}_T, \mu) < 170^\circ$, $|\Delta\phi(\cancel{p}_T, \mu) - 90^\circ|/90^\circ < \cancel{p}_T/45 \text{ GeV}$ and kinematic fit for $Z \rightarrow \mu\mu$

$^* p_T > 4 \text{ GeV}$, $\Delta R(\text{jet}, \mu) < 0.5$

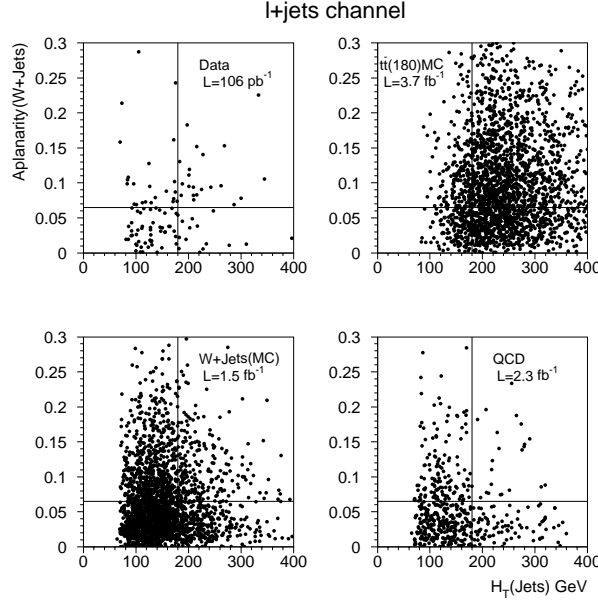


Figure 4: Distribution of $\mathcal{A}(W + \text{jets})$ vs. H_T for $\ell + \text{jets}$ events from collider data, for $W + \text{jets}$, top MC($m_t = 180$ GeV) and multijet QCD backgrounds.

We estimate the $W + \text{jets}$ background for events with high jet multiplicity by extrapolating from low jet multiplicities under the assumption that the number of $W + \text{jets}$ events falls exponentially with the number of jets in the event[6], *i.e.*,

$$N_i(W) = N_1(W)\alpha^{i-1}, \quad (1)$$

where $N_i(W)$ is the cross section for the production of a W in association with i jets, $i > 0$. We determine α from the jet multiplicity spectrum of $\ell + \text{jets}$ events that satisfy the lepton and \cancel{p}_T cuts from table 2. After subtracting the estimated multijet background we fit the multiplicity spectrum to an exponential component due to $W + \text{jets}$ and a component due to $t\bar{t}$ events,

$$N_i = N_1(W)\alpha^{i-1} + f_i N(t\bar{t}), \quad (2)$$

where N_i is the number of observed events with i jets, f_i is the fraction of $t\bar{t}$ events with i jets and $N(t\bar{t})$ is the number of $t\bar{t}$ events in the sample. α and $N(t\bar{t})$ are free parameters of the fit. The number of $W + \text{jets}$ background events in the final sample is then given by N_4 times the probability that these events survive the event shape cuts. The background estimates are summarized in table 2.

3.3 Lepton+jets b -tag analysis

The event selection for the e +jets/ μ and μ +jets/ μ channels requires an isolated high- p_T lepton, \cancel{p}_T , at least 3 jets one of which is associated with a soft muon. The criteria are listed in table 2. To reject $Z \rightarrow \mu\mu$ decays in the μ +jets/ μ channel we perform a kinematic fit to the $Z \rightarrow \mu\mu$ hypothesis. These cuts yield 5 events with an e +jets/ μ and 6 with a μ +jets/ μ final state. The expected and observed event yields are also tabulated in table 2.

The principal source of background in this analysis is W +jets production. We assume the heavy flavor content in W +jets events is the same as in multijet events. This assumption leads a slight overestimate of W +jets backgrounds, as they are expected to have a lower heavy quark content. The probability of tagging a light quark or gluon jet is given by the fraction of jets in multijet events that are tagged. This fake tagging probability is parametrized as a function of jet p_T and η . For all events that satisfy the selection criteria in table 2 except the muon-tag requirement, the probabilities for each jet to be tagged were calculated and added together to estimate the mistag background. The systematic uncertainty associated with this procedure has been studied by comparing the predicted and observed number of tags in several data samples with jet p_T thresholds varying from 20 to 85 GeV. We found the prediction to be accurate to 25%.

The background due to misidentified primary leptons is determined using our multijet data sample, which to good approximation does not contain any leptons. A detailed description of this procedure can be found in reference [4].

For the μ +jets/ μ final state we estimate the residual background due to $Z \rightarrow \mu\mu$ +jets decays, where one of the muons is counted as a tagging muon, with a Monte Carlo simulation.

Figure 5 shows the jet multiplicity spectrum of ℓ +jets/ μ events before event shape cuts. For 1 and 2 jets the observed number of events agrees with the background estimate, but for 3 or more jets an excess of events over the background estimate, indicative of $t\bar{t}$ events, is apparent.

4 Cross section

In all channels together 37 events satisfy the selection criteria. We expect 13.4 ± 3.0 events from background sources and, assuming $m_t = 180$ GeV and the calculated cross section[5], 21.2 ± 3.8 $t\bar{t}$ events. The total acceptance for $t\bar{t}$ events varies between 2% and 8% for top masses between 140 and 180 GeV.

Figure 6 shows the measured $t\bar{t}$ cross section versus top quark mass, compared to

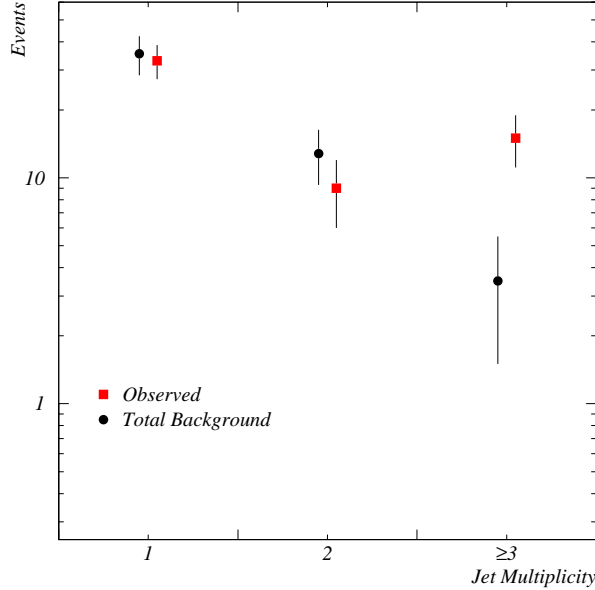


Figure 5: Jet multiplicity spectrum of ℓ +jets/ μ events before event shape cuts.

two QCD calculations[5, 12]. The error band accounts for statistical uncertainties and systematic uncertainties including the correlations between various channels.

5 $e\nu$ inclusive mode

In all modes described above we require that decay products of the t and \bar{t} are detected above momentum thresholds. This necessarily leads to inefficiencies because sometimes one of the decay products is too soft to be detected. In order to recover some of the lost efficiency we have studied a more inclusive mode. In this mode, called the $e\nu$ channel, we select events with an isolated high- p_T electron, $p_T > 50$ GeV, and two or more jets with $p_T > 30$ GeV. These events could be dilepton decays in which one of the charged leptons went undetected or misidentified or lepton+jets events in which some jets were too soft or were merged together.

The dominant background processes for $e\nu$ +jets events are $W \rightarrow e\nu$ +jets production, vector boson pairs and multijet events in which one jet fakes an electron and \cancel{p}_T is mismeasured. The W background is heavily suppressed by requiring that the transverse mass of the electron and neutrino system be greater than 115 GeV. The misidentification background is reduced by the high \cancel{p}_T cut and by requiring that the \cancel{p}_T vector not be back to back with the second leading object in the event ($|\Delta\phi - \pi| > 30^\circ$).

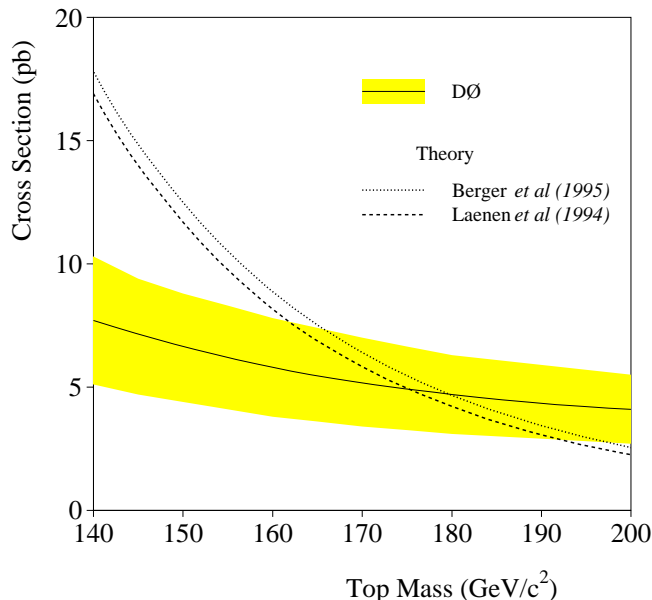


Figure 6: Top production cross section measured by the DØ experiment at the FNAL Tevatron.

In a preliminary analysis of 87.8 pb^{-1} of data two events survive the above cuts. We expect a background of 0.6 ± 0.3 events from W +jets and 0.8 ± 0.2 from multijet events leading to a total of 1.4 ± 0.4 events. For $m_t = 180 \text{ GeV}$ we expect $1.1 \pm 0.1 \text{ } t\bar{t}$ events [5]. The errors quoted for this analysis are statistical only. No systematic error estimates are available at the moment.

6 Cross section from all jets mode

For the cross section measurement in the all jets channel, we select events with six or more jets. The backgrounds from QCD multijet production is reduced by requiring the presence of at least one or two b tagged jets in the conjunction with the application of event shape variables $A(jets)$, H_T^{3j} , C and N_j^{ave} . Here $A(jets)$ is the aplanarity computed using the jets, H_T^{3j} is the scalar sum of the jet p_T excluding the leading two jets, Centrality C is the ratio of the sums of transverse and total jet energies, and N_j^{ave} is a parameter measuring the number of jets averaged over a range of p_T thresholds weighted by the p_T threshold. In an analysis of the data sample corresponding to $\approx 70 \text{ pb}^{-1}$ luminosity, we observe 15 events which have at least one b tagged jet, while 2 events survive the double b tagged analysis. The expected backgrounds for the single and doubled b tag analyses

are 11.0 ± 2.3 and 1.4 ± 0.4 events respectively. This leads to a cross section measurement of 4.4 ± 4.9 pb (single tag) and 3.9 ± 9.8 pb (double tag), which are consistent with our primary measurement from the single lepton+jets and dilepton+jets analyses.

7 Measurement of the top quark mass

One of the interesting property of the top quark is its mass, which is much higher than that of any other fermion in the Standard Model. It therefore dominates the radiative corrections to many processes. The reason for this large mass may be intimately connected with the mechanism for electroweak symmetry breaking and further study of the top quark may well shed new light on this sector of the Standard Model.

In order to perform this measurement we need to determine the response of the calorimeter to jets. We calibrate the response to light quark and gluon jets from collider data, by balancing the p_T of electromagnetic showers against jets. The energy of electromagnetic showers is well calibrated using $Z \rightarrow ee$ decays. We determine the response to b jets relative to light quark jets using a Monte Carlo simulation.

We determine the mass from lepton+jets events by performing a kinematic fit to the $t\bar{t} \rightarrow W^+(\rightarrow \ell^+\nu)b + W^-(\rightarrow q\bar{q})\bar{b}$ hypothesis. The 6 final state particles are completely specified by 18 parameters. We measure 17 of them directly. Imposing energy-momentum conservation at each vertex of the $t\bar{t}$ decay chain, ie constraining $m(\ell\nu)$ and $m(q\bar{q})$ to the W mass, and $m(W^+b)$ and $m(W^-\bar{b})$ to be equal yields 3 constraints, leading to a 2-constraint fit. That we cannot determine the identities of the jets uniquely complicates the fit. So do initial and final state gluon radiation which may give rise to additional jets. To perform the fit we assume that the four most energetic jets in the event correspond to the four quarks from the $t\bar{t}$ decay. In the absence of any information about the jet identities there are 12 ways to assign them to the four quarks plus a two-fold ambiguity for the longitudinal component of the neutrino momentum, giving a total of 24 combinations. If one jet is tagged as a b jet this reduces to 12 combinations. We fit each combination and take the χ^2 -probability weighted average of the fitted masses from up to three combinations, if $\chi^2 < 7$. This gives a slightly better resolution than retaining only the best fit, which may not always be the correct combination. This average fitted mass is not an unbiased estimator of the top mass, mainly because gluon radiation leads to biases in its value. We therefore compute the expected spectrum for this estimator as a function of the top mass from a Monte Carlo simulation of $t\bar{t}$ events with various top masses, using the HERWIG event generator. We then perform a maximum likelihood fit of these Monte Carlo spectra plus the estimated background shape to the data with the top mass as a free parameter[1].

The event selection may bias the mass spectrum of the selected event sample. In

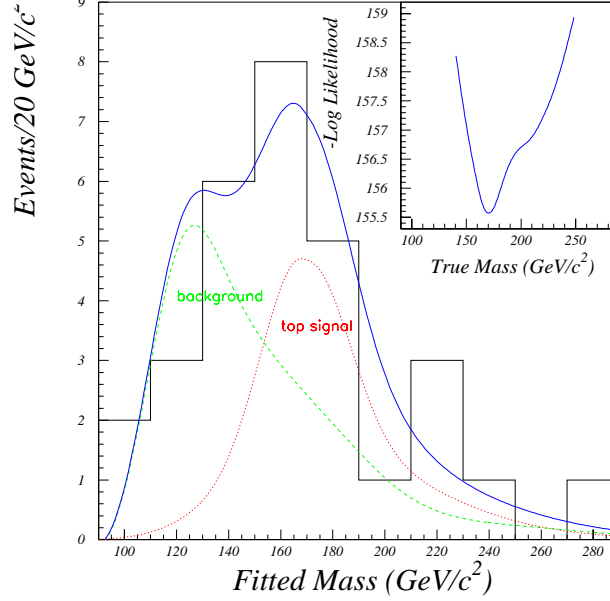


Figure 7: Mass distribution of fitted lepton+jets events. The superimposed curves are the $t\bar{t}$ signal and background components of the fit. The inset shows the log likelihood for the fit.

particular the H_T cut favors events with high mass. We therefore developed selection criteria specifically for the mass measurement that minimize this bias. We assign probabilities for events to be due to $t\bar{t}$, W +jets, or multijet production, based on the variables p_T , $\mathcal{A}(W + \text{jets})$, $(p_T(\ell) + \cancel{p}_T)/(H_T + p_T(W))$, and $\sqrt{(\sum p_T \eta^2)/(\cancel{p}_T + p_T(W))}$. We select events with an isolated high- p_T lepton, high \cancel{p}_T , and at least four jets. In our data sample we find 90 such events. Only 35 of these pass the top probability test and 30 events are successfully fitted to the $t\bar{t}$ hypothesis. Using Monte Carlo $t\bar{t}$ samples, we have verified that the spectrum of the average fitted mass is not affected by this event selection.

From the fit to the average fitted mass spectrum of the remaining 30 events we obtain

$$m_t = 170 \pm 15(\text{stat}) \pm 10(\text{syst}) \text{ GeV}/c^2. \quad (3)$$

Figure 7 shows the best fit to the average fitted mass spectrum. The statistical uncertainty is determined from Monte Carlo ensemble tests involving about 1000 MC samples of 30 events each with an average signal to background ratio of 0.42:0.58. The systematic uncertainty is due to various sources, jet energy scale ($7 \text{ GeV}/c^2$), HERWIG versus ISAJET event generator variations ($6 \text{ GeV}/c^2$), fitting procedure ($3 \text{ GeV}/c^2$), and backgrounds ($2 \text{ GeV}/c^2$).

8 Conclusion

In a data sample corresponding to 100 pb^{-1} , we observe 37 $t\bar{t}$ candidate events. The expected background is 13.4 ± 3.0 events. Using these events we measure the mass of the top quark to be $170 \pm 15(\text{stat}) \pm 10(\text{syst}) \text{ GeV}/c^2$. At this mass we find the top production cross section to be $5.2 \pm 1.8 \text{ pb}$. We also present a preliminary analysis of the alljets channel, in which the cross section measurements are consistent with the above measurement.

I would like to thank the organizers for a very interesting meeting and my DØ colleagues for their help in preparing this presentation and writeup.

References

- [1] DØ Collaboration, S. Abachi *et al.*, “Observation of the Top Quark”, Phys. Rev. Lett. **74**, 2632 (1995).
- [2] CDF Collaboration, F. Abe *et al.*, Phys. Rev. Lett. **74**, 2626 (1995).
- [3] DØ Collaboration, S. Abachi *et al.*, Nucl. Instrum. Methods **A338**, 185 (1994).
- [4] DØ Collaboration, S. Abachi *et al.*, “Top Quark Search with the DØ 1992 – 93 Data Sample”, Phys. Rev. **D52**, 4877 (1995).
- [5] E. Laenen, J. Smith, and W. van Neerven, Phys. Lett. **321B**, 254 (1994).
- [6] F. A. Berends, H. Kuijf, B. Tausk, and W. T. Giele, Nucl. Phys. B357, 32 (1991).
- [7] F. Paige and S. Protopopescu, BNL Report no. BNL38034, 1986 (unpublished), release v 6.49.
- [8] F. Carminati *et al.*, “GEANT Users Guide,” CERN Program Library, December 1991 (unpublished).
- [9] G. Marchesini *et al.*, Comput. Phys. Commun. **67**, 465, (1992).
- [10] The Random Grid Search : A simple way to find optimal cuts, N.. Amos *et al.*, DØ note 2791, Presented at CHEP’95, Rio de Janeiro, Brazil.
- [11] V. Barger, J. Ohnemus and R. J. N. Phillips, Phys. Rev. D **48**, 3953 (1993).
- [12] E. Berger *et al.*, Phys. Lett. **361B**, 115 (1995).